

A STUDY ON THE ADHESION AT A MICRO- AND NANO-LUBRICATION

Krzysztof Wierzcholski

*Technical University of Koszalin
Institute of Mechatronics, Nanotechnology and Vacuum Technique
Raclawicka Street 15-17, 75-620 Koszalin, Poland
tel.: +48 505729119, fax: +48 94 3478489
e-mail: krzysztof.wierzcholski@wp.pl*

Andrzej Miszczak

*Maritime University Gdynia, Faculty of Marine Engineering
Morska Street 81-87, 81-225 Gdynia, Poland
tel.: +48 58 6901348, fax: +48 58 6901399
e-mail: miszczak@am.gdynia.pl*

Abstract

In this paper describes the study on the adhesion forces at a nano-contact and micro- and at a nano-lubrication. Here are elaborated the dependences between oil dynamic viscosity in super thin boundary layer and adhesion forces as well influences of adhesion forces in micro- and nano-level on the friction forces in micro- and nano-scale arising between two cooperating surfaces in micro-bearings.

Up to now the influence of adhesion on oil viscosity changes and on the oil flow in micro-bearing gap was not considered in analytical way. Present paper elaborates the preliminary assumptions of hydrodynamic theory of lubrication for micro-bearing in the case if during the lubrication the adhesion forces are taking into account.

In this paper are derived the formulas of pressure distributions, friction forces and friction coefficients where the adhesion forces are considered.

The changes of adhesion forces in micro-contact of two bodies depend on the load direction. Load carrying capacity increases implied by the oil dynamic viscosity increases caused by the adhesion and cohesion forces attain about from 20% to 30% in comparison to the viscosity and capacity values in classical form.

Keywords: *adhesion forces, micro- and nano-lubrication, micro-bearings*

1. Introduction

The adhesion phenomena in recent papers had been investigated mostly in experimental way taking into account roughness of surfaces [11], nano-contact [2], ferrofluids as lubricant [7], protein coated surfaces [5], hydrate particles [1], biological surfaces [9], charged particles [6], elastic-plastic micro-contact [4], pharmaceutical particle [3, 10], polymer-polymer micro-bearings [8]. After authors knowledge, up to now the influence of adhesion on oil viscosity changes and on the oil flow in micro-bearing gap was not considered in analytical way. Present paper elaborates the preliminary assumptions of hydrodynamic theory of lubrication for micro-bearing in the case if during the lubrication the adhesion forces are taking into account. Here are presented the possibilities to derive the hydrodynamic pressure distributions, load carrying capacity, friction forces and friction coefficients in slide micro-bearings gaps taking into account the adhesion forces. We assume that the adhesion forces can to change the dynamic oil viscosity in super thin micro-bearing gap. The changes are described by the following formula:

$$\eta_T(\alpha_1, \alpha_2, \alpha_3) = \eta(\alpha_1, \alpha_3) + \eta_{adh}(\alpha_1, \alpha_2, \alpha_3). \quad (1)$$

We denote: η_T – total oil dynamic viscosity, η – classical oil dynamic viscosity, η_{adh} – oil dynamic viscosity caused by the adhesion forces. Molecules of the oil can be adsorbed on a cooperating micro-bearing surface surfaces and create high elasticity layer. Adsorption and adhesion change the dynamic oil viscosity if gap height is smaller than 1 micrometer. Fig. 1 shows the adhesion and adsorption phenomena between oil particles in micro-bearing gap.

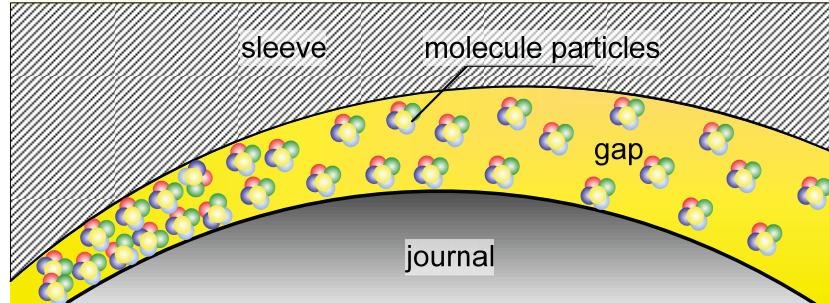


Fig. 1. Adsorption and adhesion phenomenon in micro-bearing or micro-contact gap

The groove and ridge geometry located on the conical and hyperbolic surface are presented here. Figure 2 shows that the grooves on the hyperbolic and conical journal surfaces can be situated in circumferential or longitudinal directions [2]. Groove location affects the dynamic performance of HDD spindle system.

The micro-bearing lubrication is characterized by the dynamic viscosity changes in thin gap-height direction.

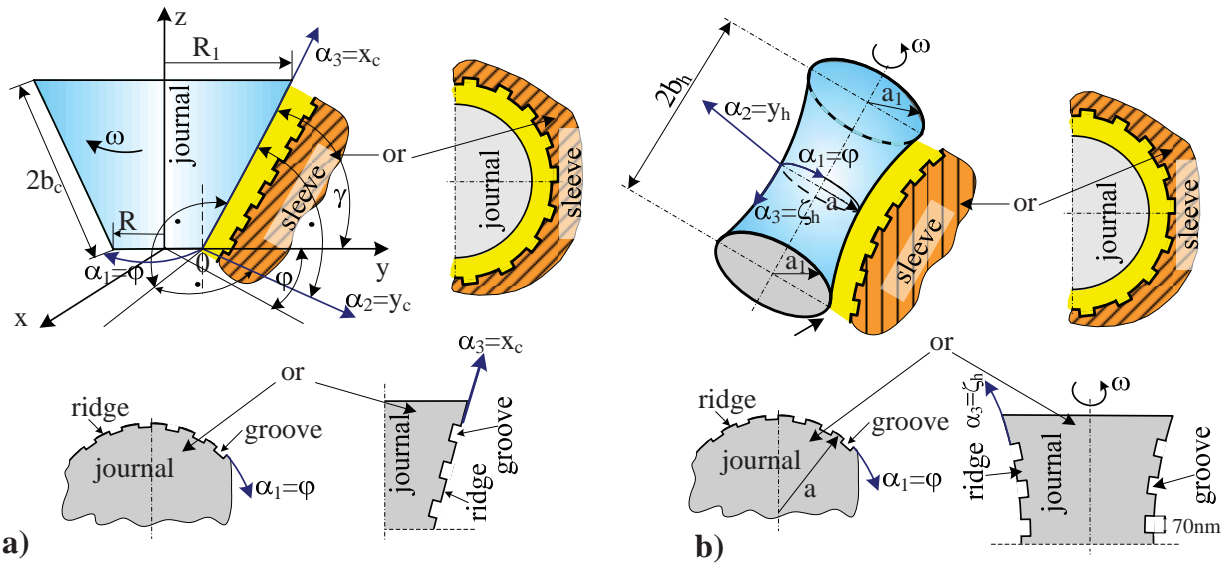


Fig. 2. The view of conical and hyperbolic micro-bearing journal surfaces: a) conical surface, b) hyperbolic surface with longitudinal and circumferential grooves, c) hyperbolic journal with grooves

2. Pressure distributions in curvilinear micro-bearings gaps

For the conical and hyperbolic micro-bearing we assume following conical and hyperbolic coordinates: $\alpha_1 = \varphi$, $\alpha_2 = y_c$, $\alpha_3 = x_c$ and $\alpha_1 = \varphi$, $\alpha_2 = y_h$, $\alpha_3 = \zeta_h$ respectively. Mentioned coordinates are presented in Fig. 2. For conical journal we assume: R_1 – the largest radius of the conical shaft, R – the smallest radius of the conical journal, $2b_c$ – the conical bearing length, γ – angle between cone generate line and the cross section plane of the journal (see Fig. 2). For hyperbolic journal we have: a_1 – the largest radius of the hyperbolic journal, a – the smallest radius of the hyperbolic

journal, $2b_h$ – the bearing length (see Fig. 2). From the system of conservation of momentum and continuity equation after thin boundary layer simplifications and boundary conditions in the curvilinear coordinates $(\alpha_1, \alpha_2, \alpha_3)$ we obtain the dimensional pressure function $p(\alpha_1, \alpha_3, t)$ satisfying the modified Reynolds equations in the following curvilinear form [6]:

$$\begin{aligned} \frac{\partial}{\partial \alpha_1} \left[\left(\frac{\partial E(p)}{\partial \alpha_1} + \frac{\partial E(p_{adh})}{\partial \alpha_1} \right) E \left(\int_0^{\varepsilon_T} A_\eta d\alpha_2 \right) \right] + \frac{h_1}{h_3} \frac{\partial}{\partial \alpha_3} \left[\frac{h_1}{h_3} \left(\frac{\partial E(p)}{\partial \alpha_3} + \frac{\partial E(p_{adh})}{\partial \alpha_3} \right) E \left(\int_0^{\varepsilon_T} A_\eta d\alpha_2 \right) \right] = \\ = \omega h_1^2 \frac{\partial}{\partial \varphi} \left[E \left(\int_0^{\varepsilon_T} A_s d\alpha_2 \right) - E(\varepsilon_T) \right] + h_1^2 \frac{\partial E(\varepsilon_T)}{\partial t}, \end{aligned} \quad (2)$$

where:

E – denotes expectancy function,

$\varepsilon_T(\alpha_1, \alpha_3, t)$ – gap height,

p_{adh} – changes of pressure caused by the adhesion.

Flow is generated by journal rotation and the sleeve is motionless. Lubricant velocity components v_1, v_2, v_3 in $\alpha_1, \alpha_2, \alpha_3$ directions, respectively, have the following form [6]:

$$v_1(\alpha_1, \alpha_2, \alpha_3, t) = \frac{1}{h_1} \left(\frac{\partial p}{\partial \alpha_1} + \frac{\partial p_{adh}}{\partial \alpha_1} \right) A_\eta + (1 - A_s) \omega h_1, \quad (3)$$

$$v_3(\alpha_1, \alpha_2, \alpha_3, t) = \frac{1}{h_3} \left(\frac{\partial p}{\partial \alpha_3} + \frac{\partial p_{adh}}{\partial \alpha_3} \right) A_\eta, \quad (4)$$

$$v_2(\alpha_1, \alpha_2, \alpha_3, t) = - \int_0^{\alpha_2} \frac{1}{h_1} \frac{\partial v_1}{\partial \alpha_1} d\alpha_2 - \int_0^{\alpha_2} \frac{1}{h_1 h_3} \frac{\partial (h_1 v_3)}{\partial \alpha_3} d\alpha_2 \quad (5)$$

and

$$A_s(\alpha_1, \alpha_2, \alpha_3, t) \equiv \frac{\int_0^{\alpha_2} \frac{1}{\eta + \eta_{adh}} d\alpha_2}{\int_0^{\varepsilon_T} \frac{1}{\eta + \eta_{adh}} d\alpha_2}, \quad (6)$$

$$A_\eta(\alpha_1, \alpha_2, \alpha_3, t) \equiv \int_0^{\alpha_2} \frac{\alpha_2}{\eta + \eta_{adh}} d\alpha_2 - A_s(\alpha_1, \alpha_2, \alpha_3, t) \int_0^{\varepsilon_T} \frac{\alpha_2}{\eta + \eta_{adh}} d\alpha_2,$$

where:

$0 \leq \alpha_2 \leq \varepsilon_T$, $0 \leq \alpha_1 < 2\pi\theta_1$, $0 \leq \theta_1 < 1$ and $0 \leq \alpha_3 \leq 2b_c$ for conical journal and $-b_h \leq \alpha_3 \leq b_h$ for hyperbolic journal,

$\eta = \eta(\alpha_1, \alpha_3)$ - liquid dynamic viscosity,

t – time.

For the conical shapes of micro-bearing journals we have following coordinates: $\alpha_1 = \varphi$, $\alpha_2 = y_c$, $\alpha_3 = x_c$, and Lamé coefficients are as follows:

$$h_1 = R + x_c \cos \gamma, \quad h_3 = 1, \quad (7)$$

where γ - angle between conical surface and the cross section plane of the journal.

For the hyperbolic shapes of micro-bearing journals we have following coordinates: $\alpha_1 = \varphi$, $\alpha_2 = y_h$, $\alpha_3 = \zeta_h$, and Lamé coefficients are as follows:

$$h_1 = a \cos^{-2}(\Lambda_{h1}\zeta_{h1}), \quad h_3 = \sqrt{1 + 4(\Lambda_{h1}/L_{h1})^2 \tan^2(\Lambda_{h1}\zeta_{h1})} \cos^{-2}(\Lambda_{h1}\zeta_{h1}), \quad (8)$$

$$\Lambda_{h1} \equiv \sqrt{\frac{a_1 - a}{a}}, \quad L_{h1} \equiv \frac{b_h}{a}, \quad \zeta_{h1} = \zeta_h / b_h,$$

where R , a , a_1 , b_h are defined before.

3. Friction forces in curvilinear micro-bearing gap

This section presents the friction forces calculation in curvilinear micro-bearing gaps. The components of friction forces in curvilinear α_1 , α_3 directions occurring in micro-bearing gaps have the following forms:

$$F_{R1} = \iint_F \left[(\eta + \eta_{adh}) \frac{\partial v_1}{\partial \alpha_2} \right]_{\alpha_2 = \varepsilon_T} h_1 h_3 d\alpha_1 d\alpha_3, \quad (9)$$

$$F_{R3} = \iint_F \left[(\eta + \eta_{adh}) \frac{\partial v_3}{\partial \alpha_2} \right]_{\alpha_2 = \varepsilon_T} h_1 h_3 d\alpha_1 d\alpha_3,$$

where:

- $0 \leq \alpha_2 \leq \varepsilon_T$, $0 \leq \alpha_1 < 2\pi\theta_1$, $0 \leq \theta_1 < 1$ and $0 \leq \alpha_3 \leq 2b_c$ for conical journal and $-b_h \leq \alpha_3 \leq b_h$ for hyperbolic journal,
- $\eta = \eta(\alpha_1, \alpha_3)$ - liquid dynamic viscosity ,
- t - time,
- F - lubrication surface,
- v_1, v_3 - fluid velocity components (3), (4) in α_1 , α_3 directions,
- h_1, h_3 - Lamé coefficients (7), (8) in α_1 , α_3 directions.

Putting formulae (3), (4) into equation (9) for curvilinear journal, then we obtain the friction components F_{R1} , F_{R3} in circumferential α_1 , and longitudinal α_3 directions, respectively:

$$F_{R1} \equiv F_{R\varphi} = \iint_F \left[\frac{\eta + \eta_{adh}}{h_1} \left(\frac{\partial p}{\partial \alpha_1} + \frac{\partial p_{adh}}{\partial \alpha_1} \right) \frac{\partial A_\eta(\alpha_1, \alpha_2, \alpha_3)}{\partial \alpha_2} \right]_{\alpha_2 = \varepsilon_T} h_1 h_3 d\alpha_1 d\alpha_3 +$$

$$- \iint_F \left[\omega h_1 (\eta + \eta_{adh}) \frac{\partial A_s(\alpha_1, \alpha_2, \alpha_3)}{\partial \alpha_2} \right]_{\alpha_2 = \varepsilon_T} h_1 h_3 d\alpha_1 d\alpha_3, \quad (10)$$

$$F_{R3} = \iint_F \left[\frac{\eta + \eta_{adh}}{h_3} \left(\frac{\partial p}{\partial \alpha_3} + \frac{\partial p_{adh}}{\partial \alpha_3} \right) \frac{\partial A_\eta(\alpha_1, \alpha_2, \alpha_3)}{\partial \alpha_2} \right]_{\alpha_2 = \varepsilon_T} h_1 h_3 d\alpha_1 d\alpha_3, \quad (11)$$

where for conical journal $F_{R3} \equiv F_{R\zeta_c}$ and for hyperbolic journal we have $F_{R3} \equiv F_{R\zeta_h}$.

If we put the functions A_s , A_η from the formulae (6) into (10), (11) then friction force components have the form:

$$F_{R1} = \iint_{\Omega} \frac{1}{h_1} \left(\frac{\partial p}{\partial \alpha_1} + \frac{\partial p_{adh}}{\partial \alpha_1} \right) \left[\varepsilon_T(\alpha_1, \alpha_3) - \frac{\int_0^{\varepsilon_T(\alpha_1, \alpha_3)} \frac{\alpha_2 d\alpha_2}{\eta(\alpha_1, \alpha_3) + \eta_{adh}(\alpha_1, \alpha_2, \alpha_3)}}{\int_0^{\varepsilon_T(\alpha_1, \alpha_3)} \frac{d\alpha_2}{\eta(\alpha_1, \alpha_3) + \eta_{adh}(\alpha_1, \alpha_2, \alpha_3)}} \right] h_1 h_3 d\alpha_1 d\alpha_3 +$$

$$- \iint_{\Omega} \left[\frac{\omega h_1^2 h_3}{\varepsilon_T(\alpha_1, \alpha_3) \int_0^{\varepsilon_T(\alpha_1, \alpha_3)} \frac{d\alpha_2}{\eta(\alpha_1, \alpha_3) + \eta_{adh}(\alpha_1, \alpha_2, \alpha_3)}} \right] d\alpha_1 d\alpha_3, \quad (12)$$

$$F_{R3} = \iint_{\Omega} \frac{1}{h_3} \left(\frac{\partial p}{\partial \alpha_1} + \frac{\partial p_{adh}}{\partial \alpha_1} \right) \left[\varepsilon_T(\alpha_1, \alpha_3) - \frac{\int_0^{\varepsilon_T(\alpha_1, \alpha_3)} \frac{\alpha_2 d\alpha_2}{\eta(\alpha_1, \alpha_3) + \eta_{adh}(\alpha_1, \alpha_2, \alpha_3)}}{\int_0^{\varepsilon_T(\alpha_1, \alpha_3)} \frac{d\alpha_2}{\eta(\alpha_1, \alpha_3) + \eta_{adh}(\alpha_1, \alpha_2, \alpha_3)}} \right] h_1 h_3 d\alpha_1 d\alpha_3, \quad (13)$$

where $0 \leq \alpha_1 \leq 2\pi\theta_1$, $0 \leq \theta_1 \leq 1$, $0 \leq \alpha_3 \leq 2b_c$, $0 \leq \alpha_2 \leq \varepsilon_T$, $\varepsilon_T = \varepsilon_T(\alpha_1, \alpha_3)$, $\eta(\alpha_1, \alpha_3)$.

Friction coefficients of conical and hyperbolic micro-bearing journals are as follows:

$$\mu_c = \frac{\sqrt{(F_{R\varphi})^2 + (F_{R\chi_c})^2}}{C_{tot}^{(c)}}, \quad \mu_h = \frac{\sqrt{(F_{R\varphi})^2 + (F_{R\zeta_h})^2}}{C_{tot}^{(h)}}, \quad (14)$$

where $C_{tot}^{(c)}, C_{tot}^{(h)}$ are the load carrying capacities in conical and hyperbolic coordinates respectively.

4. Numerical calculations

The pressure distributions and capacity values in machine conical slide micro-bearings are determined in conical coordinates: $\alpha_1 \equiv \varphi$, $\alpha_2 \equiv y_c$, $\alpha_3 \equiv x_c$, where the lubrication region Ω_c , which is defined by the following inequalities: $0 \leq \varphi \leq \varphi_k$, $0 \leq x_c \leq 2b_c$ where $2b_c$ – conical micro-bearing length.

Numerical calculations are performed in Mathcad 14 Professional Program by virtue of the equation (2) by means of the finite difference method (see Fig. 3 and 4).

The gap height of the conical micro-bearing and bio-bearing has the following form:

$$\varepsilon_T = \varepsilon(1 + \lambda_c \cos \varphi) \sin^{-1} \gamma, \quad \gamma \neq 0, \quad (15)$$

where:

λ_c - eccentricity ratio in conical micro-bearing,

ε - radial clearance of conical micro-bearing,

γ - angle between generate line and horizontal axis y .

Oil dynamic viscosity is a sum of classical viscosity and viscosity caused by adhesion and cohesion forces what is presented below:

$$\eta_T(\varphi, y_c, x_c) = \eta(\varphi, x_c) + \eta_{akh}(\varphi, y_c, x_c),$$

$$\eta_{akh}(\varphi, y_c, x_c) = a_{\eta} k + b_{\eta} \left[e^{c_{\eta}(\max(\varepsilon_T) - y_c)} + d_{\eta} e^{c_{\eta}(y_c - \max(\varepsilon_T))} \right], \quad (16)$$

$$a_{\eta} = a_{\eta\eta} \cdot \eta, \quad b_{\eta} = b_{\eta\eta} \cdot \eta,$$

where:

k - curvature (inversion of the radius of curvature),

$a_{\eta\eta}, b_{\eta\eta}, c_{\eta}, d_{\eta}$ - experimental coefficients.

The dynamic viscosity caused by adhesion and cohesion in super thin oil layer, attain the largest values near to the journal and sleeve surface in gap height direction.

Figure 3 shows the numerical pressure values in conical micro-bearing gap for the angle $\gamma = 70^\circ$ between conical surface and the cross section plane. Calculations are performed without stochastic changes for: least value of the conical journal $R = 0.001$ m, relative radial clearance $\psi = 0.002$, radial clearance $\varepsilon = 2 \cdot 10^{-6}$ m, dimensionless bearing length $L_{c1} = b_c/R = 1$, oil dynamic viscosity $\eta = 0.025$ Pas, curvature $k = 1000$ m⁻¹, experimental coefficients $a_{\eta\eta} = 0.00004$ m, $b_{\eta\eta} = 0.002$, $c_{\eta} = 3.5/\varepsilon$ m⁻¹, $d_{\eta} = 250$, angular velocity $\omega = 754$ s⁻¹, characteristic dimensional value of hydrodynamic pressure $p_o = \omega\eta R^2/\varepsilon^2$, $p_o = 4.71$ MPa, relative eccentricity values $\lambda_c = 0.4$; $\lambda_c = 0.5$.

By virtue of the boundary Reynolds conditions the angular coordinate of the film end has the values: $\varphi_k = 3.625$ rad; $\varphi_k = 3.600$ rad.

If eccentricity ratio increases from $\lambda_c = 0.4$ to $\lambda_c = 0.5$, then the maximum value of hydrodynamic pressure increases from 6.71 MPa to 14.68 MPa and total capacity in y direction increases from 11.03 N to 22.14 N and z direction increases from 4.01 N to 8.06 N.

Figures 3a and 4a show hydrodynamic pressure distributions inside conical micro-bearing gap lubricated by classical Newtonian lubricant for constant dynamic viscosity in gap height direction without changes caused by the adhesion and cohesion.

Figures 3b and 4b show hydrodynamic pressure distributions inside conical micro-bearing gap lubricated by classical Newtonian lubricant for variable dynamic in gap height direction caused by the adhesion and cohesion.

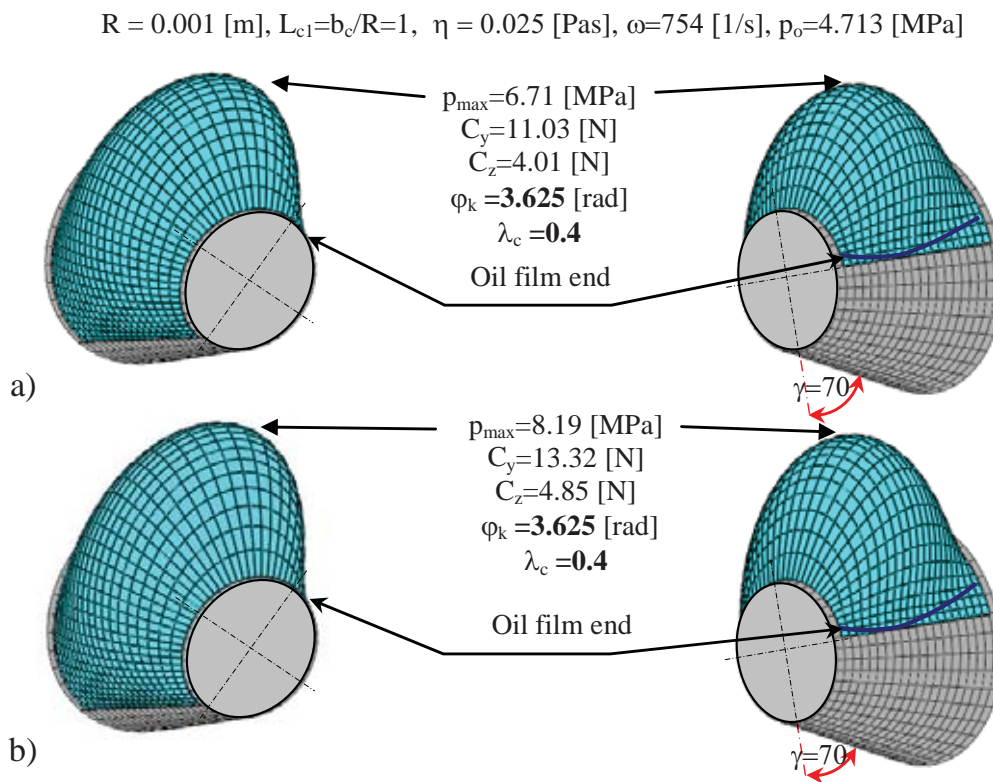


Fig. 3. The pressure distributions in conical micro-bearings caused by the rotation in circumferential direction where conical inclination angle $\gamma = 70^\circ$. Left side presents the view from the film origin, right side shows the view from film end: a) without influences of adhesion forces on the oil viscosity, b) with viscosity changes caused by the adhesion

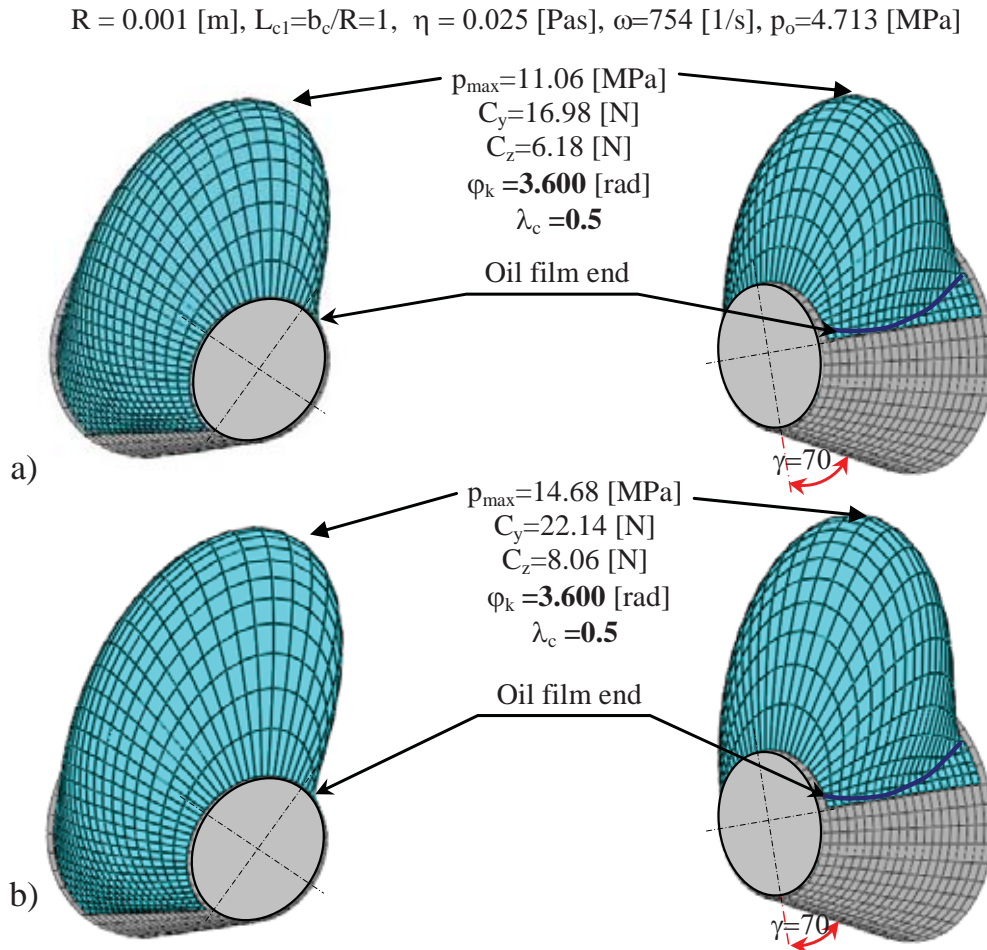


Fig. 4. The pressure distributions in conical micro-bearings caused by the rotation in circumferential direction where conical inclination angle $\gamma = 70^\circ$. Left side presents the view from the film origin, right side shows the view from film end: a) without influences of adhesion forces on the oil viscosity, b) with viscosity changes caused by the adhesion

5. Conclusions

1. Friction force increases nearly linearly with the normal load but only in case if angular velocity of the journal is very small or journal is motionless.
2. Friction force caused by the adhesion pressure existed even when the applied normal load is zero and journal is motionless.
3. Friction forces caused by the journal rotation existed if normal load is zero, adhesion forces are neglected.
4. Load carrying capacity increases implied by the oil dynamic viscosity increases caused by the adhesion and cohesion forces attain about from 20% to 30% in comparison to the viscosity and capacity values in classical form.

References

- [1] Taylor, C. J., Dieker, L. E., Miller, K. T., Koh, C. A., Dendy, S. E., *Micromechanical adhesion force measurements between tetrahydrofuran hydrate particles*, Journal of Colloid and Interface Science, Vol. 306, pp. 255-261, 2007.
- [2] Yoon, E. S., Yang, S. H., Han, H. G., Kong H., *An experimental study on the adhesion at a nano-contact*, Wear, Vol. 254, pp. 974-980, 2003.

- [3] De La Fuente, L., Montanes, E., Yizhi, M., Yaxin, L., Burr, T. J., Hoch, H. C., Mingming, W., *Assessing adhesion force of Type I and Type IV Pili of Xylella fastidiosa bacteria by use of microfluidic flow chamber*, Applied and Environmental Microbiology, Vol. 73, pp. 2690-2696, 2007.
- [4] Kogut, L., Etsion, I., *Adhesion in elastic-plastic spherical microcontact*, Journal of Colloid and Interface Science, Vol. 261, pp. 372-378, 2003.
- [5] Xu, L. C., Logan, B. E., *Adhesion forces functionalized latex microspheres and protein-coated surfaces evaluated using colloid probe atomic force microscopy*, Colloid and Surfaces B, Vol. 48, pp. 84-94, 2006.
- [6] Takeuchi, M., *Adhesion Forces of Charged Particles*, Chemical Engineering Science, Vol. 61, pp. 2279-2289, 2006.
- [7] Miranda, J. A., Oliveira, R. M., *Adhesion phenomena in ferrofluids*, Physical Review E, Vol. 70, pp. 1-11, 2004.
- [8] Rymuza, Z., Kuszniereicz, Z., Solariski, T., Kwacz, M., Chizhik, S., Goldade, A. V., *Static friction and adhesion in polimer-polymer micro-bearings*, Wear, Vol. 238, pp. 56-69, 2000.
- [9] Schwender, N., Huber, K., Marravi, F. Al., Hannig, M., Ziegler, Ch., *Initial bioadhesion on surfaces in the oral cavity investigated by scanning force microscopy*, Applied Surface Science, Vol. 252, pp. 117-122, 2005.
- [10] Tsukada, M., Irie, R., Yonemochi, Y., Nada, R., Kamiya, H., Watanabe, W., Kauppinen, E. I., *Adhesion force measurement of a DPI size pharmaceutical particle by colloid probe atomic force microscopy*, Powder Technology, Vol. 141, pp. 262-269, 2004.
- [11] Hongben, Z., Goetzinger, M., Peukert, W., *The influence of particle charge and roughness on particle-substrate adhesion*, Powder Technology, Vols. 135-136, pp. 82-91, 2003.